AT&T Technical Journal
Vol. 64, No. 4, April 1985
Printed in U.S.A.

A New Approach to Space Diversity Combining in Microwave Digital Radio

By Y. S. YEH and L. J. GREENSTEIN*

(Manuscript received May 30, 1984)

In this paper we describe a new approach to dual-channel space diversity combining in microwave digital radio. This approach features (1) adaptive control of the relative amplitudes and phases of the two branch gains; and (2) a search strategy, based on noncoherent spectrum measurements at the combiner output, that simultaneously accounts for both dispersion and noise. Computer programs have been developed to simulate the search process and to analyze the resulting performance. Eight representative channel response pairs are postulated and performance results are presented for each. They show that the scheme provides a high degree of channel equalization over bandwidths up to at least 40 MHz, and that, in receivers not using adaptive equalizers, it offers major improvements in detection performance over selection diversity.

I. INTRODUCTION

In a terrestrial digital radio link, frequency selective fading caused by multipath propagation presents the major threat to system availability. Efforts to reduce channel dispersion, and thus to increase availability, typically center on the use of adaptive equalization and/or dual-branch space diversity.[1-11]

Most conventional space diversity schemes use either selection switching or so-called "in-phase" combining of the diversity branches. The latter approach concentrates on maximizing the combiner output power rather than on minimizing channel dispersion. Recent work,

* Authors are employees of AT&T Bell Laboratories.

however, has dealt with "out-of-phase" combining, which reduces output dispersion by suitably adjusting the relative phases between the two branches.[4,8] This approach can completely eliminate dispersion for certain two-path propagation situations, but not under more general and realistic conditions.

In this paper, we describe a combiner in which the relative phases *and* amplitudes of the two branches are controlled. With little increase in complexity, this approach allows the effects of both dispersion and noise to be jointly minimized. We shall consider this type of combining within the context of M-level Quadrature Amplitude Modulation (M-QAM) systems.

Two specific approaches for finding the best amplitude and phase adjustments are described in Section II. One in particular, based on noncoherent spectrum measurements at the combiner output, is identified for further study. The simulation and analysis of this scheme are discussed in Section III, and its performance for several postulated dual-channel response pairs is assessed in Section IV. Comparisons with other diversity and nondiversity approaches are also given and attest to the effectiveness of the new scheme.

II. THE DIVERSITY COMBINER

2.1 Rationale

The idea of using both amplitude and phase adjustments in space diversity combining, while not entirely new, has yet to be fully understood and optimally exploited. We now illustrate the potential power of this form of combining under quite general circumstances. To do so, we will invoke some recent work on the modeling and analysis of multipath fading responses.

Let $H_1(f)$ and $H_2(f)$ be the complex frequency responses of a fading channel as viewed by two vertically spaced receiver antennas. Under nonfading conditions, these functions are flat with frequency at unity amplitude ($|H_1(f)| = |H_2(f)| = 1$). In all that follows, we measure f from the center of the radio channel, so that $H_1(f)$ and $H_2(f)$ are baseband functions. Moreover, we are interested in their variations over just the interval $[-W/2, W/2]$, where W is the channel bandwidth in hertz. Since multipath fading arises from a finite number of discrete propagation paths, we can present $H_1(f)$ and $H_2(f)$ in the following general forms:

$$H_1(f) = \sum_{k=1}^{K_1} R_{1k}\exp\{-j(\omega\tau_{1k} - \theta_{1k})\} \tag{1}$$

and

$$H_2(f) = \sum_{k=1}^{K_2} R_{2k}\exp\{-j(\omega\tau_{2k} - \theta_{2k})\}. \tag{2}$$

In (1), K_1 is the number of paths and τ_{1k}, R_{1k}, and θ_{1k} are the time delay, amplitude, and phase, respectively, associated with the kth path. Similar definitions apply to K_2, τ_{2k}, R_{2k}, and θ_{2k} in $H_2(f)$.

Typically, multipath propagation on microwave radio links exhibits delay spreads on the order of 10 ns or less, i.e., the largest and smallest τ values differ by amounts small compared to $1/W$, where $W \leqslant 40$ MHz in the common carrier bands. This observation inspired earlier efforts to approximate fading channel responses using low-order polynomials in $j\omega$.[12]

To be concrete, let $H_1(f)$ and $H_2(f)$ be represented by the infinite power series

$$H_1(f) = e^{-j\omega t_1}[A_1 + j\omega B_1 + (j\omega)^2 C_1 + \cdots] \tag{3}$$

and

$$H_2(f) = e^{-j\omega t_2}[A_2 + j\omega B_2 + (j\omega)^2 C_2 + \cdots], \tag{4}$$

where t_1 and t_2 are arbitrary, and the A's, B's, and so on are complex coefficients. Using the power series expansion for e^{jx}, they can be easily related to the parameters of the functions (1) and (2), e.g.,

$$A_1 = \sum_{k=1}^{K_1} R_{1k} e^{j\theta_{1k}}; \qquad B_1 = \sum_{k=1}^{K_1} R_{1k} e^{j\theta_{1k}}(t_1 - \tau_{1k}), \tag{5}$$

and so on.

The essence of *first-order* polynomial fitting is this: Given $H_1(f)$, a value for t_1 can usually be found such that $(A_1 + j\omega B_1)$ is the dominant part of (3) over $[-W/2, W/2]$, all higher-order terms in $j\omega$ being small, in some sense. Similarly, a value for t_2 can usually be found that does the same for $H_2(f)$, (4). That such first-order polynomial fitting is reasonable to do in common carrier channels has been supported by theory,[13] noncoherently measured data,[12] and (more recently) coherently measured data.[14]

Now suppose that a space diversity combiner were used having an adjustable time delay (τ) and complex gain (β) in the second branch. The composite channel response, as viewed at the combiner output, would then be

$$H(f) = H_1(f) + \beta e^{-j\omega\tau} H_2(f). \tag{6}$$

If τ and β were adaptively adjusted to be

$$\tau = t_1 - t_2 \quad \text{and} \quad \beta = -B_1/B_2, \tag{7}$$

we could then write [see (3) and (4)]

$$H(f) = [A_1 - A_2 B_1/B_2] + \left\{\begin{matrix}\text{second- and} \\ \text{higher-order} \\ \text{terms in } j\omega\end{matrix}\right\}. \tag{8}$$

Thus, by proper choice of delay and gain in one branch, the channel response could be made dispersionless except for small higher-order terms in $j\omega$. This is a quite general result for the channels of interest and shows the power of the combining approach under study. If β were a phase-only factor [$\beta = \exp(j\phi)$], such a strong reduction in dispersion would only be possible in those fortuitous situations where $|B_1| = |B_2|$.

2.2 The combiner structure

The above discussion suggests both a particular structure, (6), for the combiner and particular solutions, (7), for the variable parameters. The discussion was intended, however, to provide insight rather than to identify a serious design approach. For one thing, a variable time delay would be difficult to implement and would offer little incremental benefit in most cases. In addition, the solutions of (7) do not properly address either the residual dispersion (i.e., higher orders in $j\omega$) or the receiver noise. If, for example, A_1/B_1 and A_2/B_2 happened by chance to be close in value, the first term in (8) would be severely weakened in the process of eliminating the $j\omega$ term; this would enhance the effects of both the remaining dispersion and the noise.

Accordingly, we propose a combiner in which the relative amplitudes and phases in the two diversity branches are adaptively adjusted, but not the delays. Thus,

$$H(f) = \beta_1 H_1(f) + \beta_2 H_2(f), \tag{9}$$

as indicated in Fig. 1, where β_1 and β_2 are adapted gains. (Because the dominant thermal noise is introduced before the combiner, several ways of adapting β_1 and β_2 would, in theory, yield equivalent performance. For example, one gain could be held fixed, or adapted in amplitude only, with the other being adapted in both amplitude and phase; or both gains could be adapted in both amplitude and phase. Each of these approaches would permit the adaptation of the *relative* complex branch gains, which is all that matters.) Moreover, we propose the use of control strategies that take proper account of both dispersion and noise.

2.3 Control strategies

We shall discuss two distinct approaches for controlling the gain pair (β_1, β_2) in (9). The first approximates the theoretically best way to do combining when there is no post-combiner equalization. The second approach, thought suboptimal, has features that make it attractive both with and without post-combiner equalization. The new scheme reported here incorporates the second approach, whose performance we will compare with that of the first.

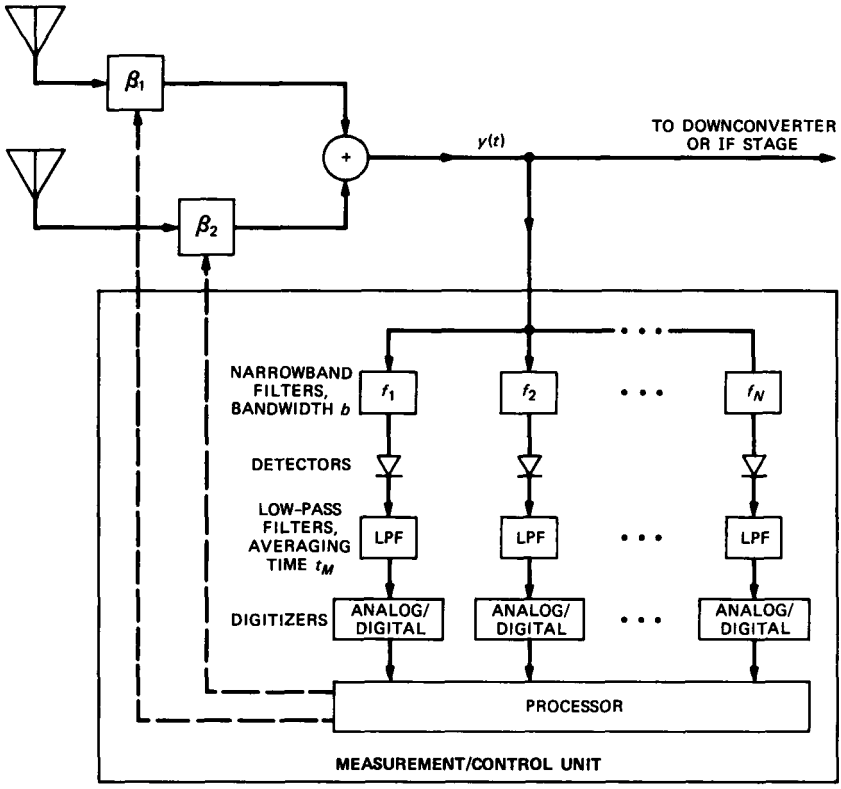

Fig. 1—Block diagram of the space diversity combiner. In this scheme, noncoherent spectral measurements are made on the combiner output at three or more inband frequencies, and the control measure formed from them is used to adjust the complex gains β_1 and β_2. The combining is shown at Radiofrequency (RF) but could be at Intermediate Frequency (IF) instead.

Approach 1: Assume for now that there is no post-combiner equalization. In that case, the detection bit error rate is virtually minimized by choosing (β_1, β_2) to maximize the ratio of sampled signal to root mean squared (rms) distortion at the receiver output. By "sampled signal," we mean the half-distance between signal levels, as sampled in every period at the in-phase and quadrature detectors; by "rms distortion," we mean the rms sum of thermal noise and Intersymbol Interference (ISI) sampled at the detectors. This signal-to-distortion ratio [defined formally by (26) and expressed by (28), below] depends on $H_1(f)$, $H_2(f)$, β_1, β_2, and other factors; most important, it is convex in β_1 and β_2. The result is that there is a unique value of relative complex gain, β_1/β_2, that maximizes this ratio. We shall regard as *optimal* any gain pair (β_1, β_2) that exhibits this maximizing relative gain.

There is a practical way to realize optimal values for β_1 and β_2,

namely, gradient search methods using data decisions.[15,16] The action is similar to that of an adaptive transversal equalizer, with β_1 and β_2 taking the place of the optimized tap gains. We shall refer to this or any decision-directed scheme that optimizes (β_1, β_2), in the sense defined above, as Approach 1.

Approach 2: A potential liability of Approach 1 is that it relies on having accurate data decisions, a condition that may not always exist (e.g., during recovery from severe fades). The scheme to be reported here is based on a different strategy, which we designate as Approach 2. It consists of (1) performing certain noncoherent spectral measurements on the combiner output; and (2) sequentially searching over (β_1, β_2) so as to maximize a certain quantity [eq. (18), below] computed from these measurements. By adapting β_1 and β_2 in this way, a close approximation to the "optimal" condition defined above can be achieved, as we show later. That is, Approach 2 should yield near-optimal detection performance for receivers having no post-combiner equalization. For cases where such equalization *is* used, Approach 2 would serve a different purpose—reducing the signal dispersion as seen by the equalizer input, thereby simplifying the requirements on equalizer design (e.g., number of taps) and improving convergence speed. Thus, Approach 2 has the twin virtues of not relying on data decisions and having utility both with and without post-combiner equalization.

To describe Approach 2, we refer to the block diagram of Fig. 1. The combiner output signal, $y(t)$, has a power spectrum density given by

$$S_y(f) = \underbrace{S(f)\,|H(f)|^2}_{\text{Signal}} + \underbrace{N_o(|\beta_1|^2 + |\beta_2|^2)|H_R(f)|^2}_{\text{Noise}}, \qquad (10)$$

where N_o is the power spectrum density of the receiver input noise,* $H_R(f)$ represents whatever receiver selectivity precedes the combiner output, and $S(f)$ is the spectral density of the signal (excluding channel and combiner effects). More specifically,

$$S(f) = S_o|H_T(f)|^2|H_R(f)|^2, \qquad (11)$$

where $|H_T(f)|^2$ represents the spectral shaping in the transmitter and S_o is a spectral density scale factor.

All functions and parameters in (10) and (11) are design-specified except $|\beta_1|$ and $|\beta_2|$, which are controlled by the combiner circuitry, and $|H(f)|$, which must be measured in real time. Our scheme estimates $|H(f)|$ at N evenly spaced frequencies (N odd) within the

* Though not made explicit by the figure, we assume there is sufficient front-end amplification that the combiner gains β_1 and β_2 have no effect on receiver noise figure.

channel bandwidth by estimating the corresponding values of $S_y(f)$ [see eq. (10)]. Based on these estimates, β_1 and β_2 are adjusted to maximize a computed performance measure, Y, which we introduce shortly. Before doing so, we define the following:

$$\Delta f \triangleq \text{Spacing between estimates of } |H(f)|, \tag{12}$$

where $(N-1)\Delta f \leqslant W$;

$$H_n \triangleq |H(f_n)|, \qquad f_n = n\Delta f\,(n = 0, \pm 1, \cdots \pm (N-1)/2); \tag{13}$$

$$\bar{H} \triangleq \underset{n}{\text{Ave}}\{H_n\} = \text{“Average Signal Gain”}; \tag{14}$$

$$X_{\text{sig}} \triangleq \underset{n}{\text{Ave}}\{S(f_n)\}(\bar{H})^2 W = \text{“Signal Power”}; \tag{15}$$

$$X_{\text{dis}} \triangleq \underset{n}{\text{Ave}}\{S(f_n)(H_n - \bar{H})^2\} W = \text{“Distortion Power”}; \tag{16}$$

$$X_{\text{noise}} \triangleq N_o(|\beta_1|^2 + |\beta_2|^2)\underset{n}{\text{Ave}}\{|H_R(f_n)|^2\} W = \text{“Noise Power”}; \tag{17}$$

where W and T are the channel bandwidth and digital symbol period, respectively. All quantities in these equations are known a priori except the H_n values, which are measured.

We now define the performance measure to be computed and maximized, namely,

$$Y \triangleq X_{\text{sig}}/(X_{\text{dis}} + X_{\text{noise}}). \tag{18}$$

This ratio is an approximation, computed from noncoherent spectral measurements, of the detector output signal-to-distortion ratio defined by (26), below. It is an apt measure to maximize in its own right, for the following reasons: In typical digital radio links, noise will not be a serious factor unless $H_1(f)$ and $H_2(f)$ are strongly faded. Therefore, maximizing Y will, in most cases, amount to minimizing the ratio $X_{\text{dis}}/X_{\text{sig}}$, which is a measure of the dispersion in $H(f)$. Including X_{noise}, however, safeguards against minimizing this ratio at an undue cost in signal (X_{sig}) and thus seriously degrading the signal-to-noise ratio.

The control strategy is therefore as follows (see Fig. 1): At the combiner output, a parallel bank of envelope detectors is used to estimate $|H(f)|$ at N frequencies. The spectral samples are digitized and applied to a microprocessor, which computes Y. This measure drives the search over $|\beta_1|$ (*or* $|\beta_2|$) and $\phi = \text{Arg}\{\beta_2\}$, i.e., these quantities are adjusted so as to maximize Y. Typically, they are adjusted iteratively, e.g., ϕ is changed in 0.1-radian step until a local maximum is found; then $|\beta_1|$ or $|\beta_2|$ is changed from 1 in steps of 0.1 until a maximum is found; and this process repeats, possibly using smaller steps in successive rounds, until Y can no longer be increased

by varying either β or ϕ. If each measurement (i.e., set of estimates of $|H(f)|$ at N frequencies) and computation for Y takes t_M seconds, and N_A steps are needed to find (β_1, β_2), then the "solution time" of the combiner will be about $N_A t_M$. This number should be small compared to 1 second to achieve timely adaptation to multipath fades.

2.4 Measurements

We now discuss the scheme for measuring the set of H_n's in (13). In our simulations (Section III) we treat only the case where $N = 3$ and $\Delta f = W/2$ (i.e., three samples, taken at the channel edges and center). In practice, the outer samples would probably be closer-in so as to minimize errors from adjacent-channel interference. Also, higher values of N (e.g., $N = 5$) might be worthwhile.

To see how accurate estimates of H_n might be obtained, let $G(f)$ represent a low-pass power gain function with bandwidth $b/2 \ll W$. We envision the measurement of H_n as involving a bandpass filter with power response $G(f - n\Delta f)$ followed by envelope detection and t_M-second averaging of the detector output (Fig. 1). Referring to eq. (10), the average power at the output of the bandpass filter will be

$$\bar{P}_n = \int \{S(f)|H(f)|^2 + N_o(|\beta_1|^2 + |\beta_2|^2)|H_R(f)|^2\}G(f - n\Delta f)df, \quad (19)$$

where $S(f)$ is defined by (11). Assuming a square-law detector, the time-averaged detector output will be

$$\langle \bar{P}_n \rangle = \bar{P}_n + \left\{\begin{matrix}\text{Fluctuation Noise;} \\ \text{Variance} \sim \bar{P}_n/bt_M\end{matrix}\right\}. \quad (20)$$

We now define two constants related to the system design functions, namely,

$$\eta_n \triangleq N_o \int |H_R(f)|^2 G(f - n\Delta f)df \quad (21)$$

and

$$\zeta_n \triangleq \int S(f)G(f - n\Delta f)df. \quad (22)$$

Based on (19) and the fact that $H(f)$ changes little over the bandwidth b, a microprocessor can estimate H_n using the formula

$$\hat{H}_n = \sqrt{\frac{\langle \bar{P}_n \rangle - \eta_n[|\beta_1|^2 + |\beta_2|^2]}{\zeta_n}}, \quad (23)$$

where $\langle \bar{P}_n \rangle$ is measured in real time; $|\beta_1|$ and $|\beta_2|$ are controlled parameters of known value; and η_n and ζ_n are predetermined constants.

Equation (23) shows how $\hat{H}_n$ is computed in terms of measured or known quantities. To see what this computed number represents, we insert (19) through (22) into (23) and obtain

$$\hat{H}_n = \sqrt{\frac{\int S(f)G(f - n\Delta f)|H(f)|^2 df}{\int S(f)G(f - n\Delta f)df} + \left\{\begin{matrix}\text{Term due solely to} \\ \text{fluctuation noise}\end{matrix}\right\}}. \quad (24)$$

We can now cite choices for b and t_M that lead to accurate and sufficiently rapid estimations of H_n. As b gets very small, the first term under the radical sign in (24) approaches H_n^2, so that the major inaccuracy in $\hat{H}_n$ is due to fluctuation noise. To be more precise, the first term is close to H_n^2 so long as $|H(f)|^2$ changes little over the passband of $G(f - n\Delta f)$. Since we are considering propagation media with delay spreads of just a few nanoseconds, the design rule $b \leq 2$ MHz should permit more than adequate resolution in this regard. To achieve low mean-square fluctuation noise as well [second term in (24)], the condition $bt_M \geq 4000$ should be satisfied [see (20)]. Thus, with $b = 2$ MHz and $t_M = 2$ ms, H_n can be approximated with high accuracy by the quantity $\hat{H}_n$. Moreover, this design choice would permit numerous iterations of the search over β_1 and β_2 before the medium response changes appreciably.

III. PERFORMANCE STUDY

3.1 General

We have written a set of computer programs to simulate the behavior of the combiner scheme described above (Approach 2) and to analyze its performance and that of other receiver techniques. Each simulation is done for a specific pair of fading functions, $H_1(f)$ and $H_2(f)$, and for a specific value of Carrier-to-Noise Ratio (CNR). What is simulated is the sequential search over β_1 and β_2, as performed by a receiver in real time to maximize the computed measure Y [see eq. (18)].

The analysis programs compute a detection performance measure for a nonequalized receiver using the (β_1, β_2) pairs derived in the simulations for Approach 2. The same measure is also computed for the cases of *optimal* combining (Approach 1) and no combining (nondiversity). Also, the analysis programs examine the signal dispersion at the combiner output for these various cases, which has relevance to receivers with post-combiner equalization.

3.2 Response pairs studied

We have specified eight distinct pairs of $H_1(f)$ and $H_2(f)$ for purposes of study. These pairs are collectively representative of what

Table I—Dual-channel response pairs studied

CASE	PLOTS OF $\lvert H_1(f)\rvert, \lvert H_2(f)\rvert$ (IN dB)	SPACE DIVERSITY CHANNEL	PATH NUMBER, k	τ_k (IN ns)	$R_k \exp(j\theta_k)$
1	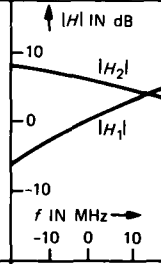	1	1	-4.0	1.0 + j0.1
			2	+1.0	-0.5 + j0.9
		2	1	-2.0	1.1 + j0.4
			2	+4.0	0.9 - j0.4
2	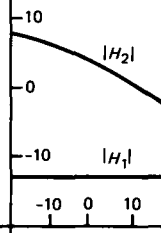	1	1	-4.0	0.2 + j0.1
		2	1	-5.0	-1.1 + j0.6
			2	+3.0	0.5 + j1.1
3	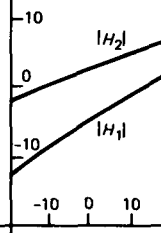	1	1	-1.0	1.0 + j0.1
			2	+2.0	-0.9 + j0.5
		2	1	-2.0	1.1 + j0.9
			2	+2.0	-1.0 + j0.5
4	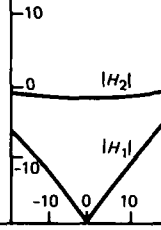	1	1	-1.0	1.0 + j0.0
			2	+2.0	-0.9 + j0.0
		2	1	-2.0	1.1 + j0.0
			2	+2.0	-0.5 + j0.0

might arise in actual radio links using space diversity. In each case, $H_1(f)$ corresponds to a one-, two- or three-path medium, and similarly for $H_2(f)$. [In terms of (1) and (2), $K_1 = 1$, 2, or 3 in each case, and similarly for K_2.] The corresponding time delays and complex gains are summarized in Table I. Also shown for each case are graphs of $|H_1(f)|$ and $|H_2(f)|$, in decibels, over a 40-MHz bandwidth.

Table I—(Cont.) Dual-channel response pairs studied

CASE	PLOTS OF $\lvert H_1(f)\rvert$, $\lvert H_2(f)\rvert$ (IN dB)	SPACE DIVERSITY CHANNEL	PATH NUMBER, k	τ_k (IN ns)	$R_k \exp(j\theta_k)$
5	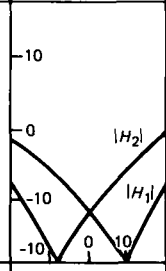	1	1 2	-2.0 +2.0	1.0 + j0.0 -0.872 - j0.223
		2	1 2	-1.0 +3.0	0.54 + j0.84 -0.66 - j0.60
6	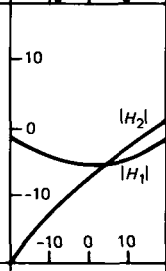	1	1 2	-3.0 +3.0	1.0 + j0.0 -0.5 + j0.0
		2	1 2	-3.0 +1.0	-0.068 - j0.998 0.48 + j0.76
7	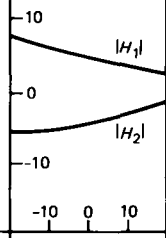	1	1 2 3	-3.0 0.0 +2.0	0.0 - j1.0 0.5 + j0.5 1.0 + j0.0
		2	1 2 3	-3.0 0.0 +2.0	0.0 - j1.0 -0.5 + j0.5 0.5 + j0.0
8	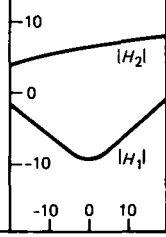	1	1 2 3	-3.0 -1.0 +2.0	-1.0 + j0.5 0.2 + j0.7 0.5 - j1.0
		2	1 2 3	-2.0 +1.0 +2.0	1.0 - j0.2 1.0 - j0.2 0.5 + j0.5

Because of additive noise, the receiver performance for a given response pair would be affected by any amplitude scaling of $(H_1(f), H_2(f))$. We permit the possibility of such a scaling, for each case in Table I, by including it in the carrier-to-noise ratio parameter discussed below.

3.3 Signal design assumed

We assume throughout the study that the signal spectral density $S(f)$, (11), is rectangular over the channel bandwidth, with magnitude S_o. This corresponds to the use of ideal Nyquist pulses with 0-percent roll-off factor ($\alpha = 0$) and a symbol rate equal to the bandwidth ($1/T = W$). While not realistic, this assumption both simplifies the analysis and leads to somewhat poorer results than for other (more tapered) spectra.[17] It thus serves both convenience and our confidence in whatever favorable outcome the study predicts. Adding to the "worst-case" nature of the results is that they are obtained for the largest common carrier channel bandwidth, $W = 40$ MHz.

3.4 Carrier-to-noise ratio

Finally, we introduce a so-called flat fading gain, g, with which we can amplitude-scale the various pairs $(H_1(f), H_2(f))$ in Table I. Accordingly, we define the flat-fading carrier-to-noise ratio to be

$$\text{CNR} \triangleq g^2 S_o / N_o. \tag{25}$$

A typical system value for this quantity, with $g^2 = 1$, is 10^6 (60 dB). We will consider a wide range of values for CNR, thereby accommodating a wide range of amplitude scaling factors.

3.5 Method of analysis

We consider an M-level QAM system with the previously noted Nyquist signaling. At each baseband detector, data decisions are made every T seconds by comparing the sampled input with a set of decision thresholds. We now introduce the following new quantities:

$P_S \triangleq$ The squared signal sample (excluding ISI and noise) at either baseband detector, when a data value of +1 or −1 is being detected;

$P_I, P_N \triangleq$ The mean-squared ISI and noise, respectively, associated with the periodic samples at either baseband detector.

We define the detection signal-to-distortion ratio to be

$$\rho_D \triangleq P_S / (P_I + P_N) \tag{26}$$

and note that this quantity yields a reasonably tight upperbound to the bit error rate, via[18]

$$\text{Bit Error Rate} \leq 2 \exp(-\rho_D/2). \tag{27}$$

We thus regard ρ_D as a proper index for evaluating digital radio receiver performance.

Now consider a space diversity receiver using no post-combiner equalization and exhibiting a channel response $H(f)$, (9), at the

combiner output. For the assumed M-QAM system, with optimal timing and carrier recovery, we can show that

$$\rho_D = \frac{3}{M-1} \frac{\mathrm{CNR}(H_{\max}^2)}{\mathrm{CNR}(\overline{|H|^2} - H_{\max}^2) + (|\beta_1|^2 + |\beta_2|^2)} \equiv \frac{3}{M-1}\Gamma, \quad (28)$$

where

$$H_{\max} \triangleq \operatorname*{Max}_{t_o} \left| T \int_{-W/2}^{W/2} H(f) e^{-j\omega t_o} df \right| \quad (29)$$

and

$$\overline{|H|^2} \triangleq T \int_{-W/2}^{W/2} |H(f)|^2 df. \quad (30)$$

Note that the dependence of ρ_D on M resides entirely in the factor $3/(M-1)$. By using Γ as our signal-to-distortion measure, therefore, we can remove M from the set of problem variables.

Since $H(f)$ is linear in β_1 and β_2, a solution exists for these gains (actually, for their *ratio*) that maximizes Γ. The solution can be found analytically by a variation on the method outlined in Section 5.1 of Ref. 15. In an actual receiver, the solution can be closely realized using practical circuitry, which we have designated as Approach 1 (Section 2.3). This solution for (β_1, β_2) is defined here to be optimal, and we will compute and present Γ results corresponding to it. These will be compared with Γ results for the "suboptimal" (β_1, β_2), which we define as the pair produced under Approach 2 (Section 2.3) and which are obtained here via computer simulations. For completeness, we will also show Γ results for the case of no diversity, i.e., either $\beta_1 = 1$, $\beta_2 = 0$ (Branch 1 only is processed) or $\beta_1 = 0$, $\beta_2 = 1$ (Branch 2 only is processed).

Finally, in consideration of receivers using post-combiner equalization, we define a "dispersion index" for $H(f)$ as follows:

$$R \triangleq \left[\frac{\operatorname*{Max}_f \{|H(f)|\}}{\operatorname*{Min}_f \{|H(f)|\}} \right] |f| \leq 20 \text{ MHz}. \quad (31)$$

This is just the *range* of $|H(f)|$ over a 40-MHz channel bandwidth. Gersho has shown that adaptive equalizers converge more rapidly when this ratio is close to unity.[19] Another likely benefit of near-unity R is that effective equalization should be attainable using a relatively small number of equalizer taps. We will compute R for the same cases that we compute Γ.

3.6 *Simulation of the search algorithm for Approach 2*

The simulations assume three spectrum measurements located at −20 MHz, 0 MHz, and +20 MHz relative to the band center. As noted before (Section 2.4), we can identify design parameters that drive measurement inaccuracies to negligible levels. For this reason, we assume exact spectral estimates and have not attempted to simulate measurement inaccuracies.

For a given response pair (Table I) and CNR, (24), the simulation proceeds as follows: During the search process one of the β values is always set to unity with the other value less than or equal to unity. Initially, $|\beta_1|, |\beta_2|$ and ϕ are set to 1.0, 1.0 and 0, respectively. Then ϕ is varied in $\delta\phi$-radian steps until Y, (18), is maximized. Next, $|\beta_2|$ is varied in steps of $\delta\beta$ (if the simulation calls for increasing $|\beta_2|$ above unity, we set $|\beta_2| = 1$ and decrease $|\beta_1|$ instead) until Y is again maximized. The procedure is then repeated until Y cannot be further maximized.

In the simulations, we generally started with $\delta\beta = 0.1$ and $\delta\phi = 0.1$ radian. We noticed that a steady-state result usually required about twice the number of steps needed to reach it directly. For example, if the solution were $|\beta_1| = 1.0$, $|\beta_2| = 0.4$, and $\phi = 3.1$ radians, a "direct" path would entail six 0.1-step changes in $|\beta_2|$ and 31 0.1-radian changes in ϕ, or 37 steps in all. The maximizing algorithm described above, however, was found to take about 74 steps. Using $\delta\beta = 0.01$ and $\delta\phi = 0.01$ radian would, of course, require 740 steps. Our approach was to use 0.1 for both increments until a stable solution was reached and then to proceed to a finer solution by changing both increments to 0.01. The end results using this faster two-stage process were identical to those obtained by using 0.01 throughout.

Using the two-stage process, the measurement steps needed to reach a solution should not exceed perhaps 200 for a "cold start" adjustment of the combiner gains. For $t_M = 2$ ms per measurement, this corresponds to a solution time of 0.4 second. In the dynamic situation where the receiver tracks the channel variations, the solution time would be much shorter.

An important question is whether the derived solutions for (β_1, β_2) are unique. We explored this question for each of the eight cases in Table I, plus a few others. For each case, we simulated the search process using 24 different starting points for $|\beta_1|$, $|\beta_2|$ and ϕ. Specifically, $(|\beta_1|, |\beta_2|)$ was initialized to each of three different pairs of values, namely, (0.5, 1.0), (1.0, 1.0), and (1.0, 0.5); and, for each such pair, ϕ was initialized to each of eight values, namely, 0, 45, 90, $\cdots$ 315 degrees. In studying the 24 solutions for each case, we observed:

1. The solution for (β_1, β_2) was not unique in every case; for some cases, multiple local maxima for Y were found to exist, and the search

algorithm converged to one or another, depending on the starting point.

2. The multiple-solution condition appears to exist only at high CNR ($\geq$40 dB); for CNR = 20 dB, all solutions for (β_1, β_2) were found to be unique.*

3. In those cases where multiple solutions *did* exist, the lowest of the resulting Y values was always quite good (>30 dB) and usually not much below the highest Y.

From these observations, we tentatively conclude that the proposed scheme converges to stable solutions under all circumstances. Further, the solutions seem to be nonunique only in circumstances where all of the possible solutions are satisfactory.

IV. RESULTS

A qualitative assessment of the combining scheme can be gained using graphical results. Figures 2, 3, and 4 show, for each of Cases 1, 3, and 4 in Table I, plots of $H_1(f)$, $H_2(f)$, and the $H(f)$ obtained when CNR = ∞. In each figure, the severe dispersions of $H_1(f)$ and $H_2(f)$ are seen to be almost eliminated by the combining: $H(f)$ presents a nearly flat amplitude response and a nearly linear phase response over the channel bandwidth.

To make the assessments more quantitative, we have computed Γ and R, (28) and (31), for each case in Table I; for each of the CNR values 60 dB, 40 dB, and 20 dB; and for each of the following four solution strategies for (β_1, β_2):

Solution 1: Optimal; based on Approach 1, it leads to a maximum for Γ with respect to β_1 and β_2.

Solution 2: Suboptimal; based on Approach 2, it leads to a maximum for Y with respect to β_1 and β_2.†

Solution 3: Nondiversity; Branch 1 processed only.

Solution 4: Nondiversity; Branch 2 processed only.

We define Γ_i and $R_i (i = 1, 4)$ to be the decibel values of Γ and R, respectively, for Solution 1. The results are given by Tables II, III, and IV, each corresponding to one of the three values of CNR.

V. DISCUSSION AND CONCLUSION

The data of Tables II through IV lead us to the following observations:

1. Comparing Γ_2 with Γ_3 and Γ_4 reveals that an unequalized receiver

* Under low CNR conditions, the noise term dominates. Since the noise term is quadratic in β_1 and β_2, it leads to a unique maximum for Y.

† In all cases where multiple solutions were found to exist, we used the one corresponding to the higher Y.

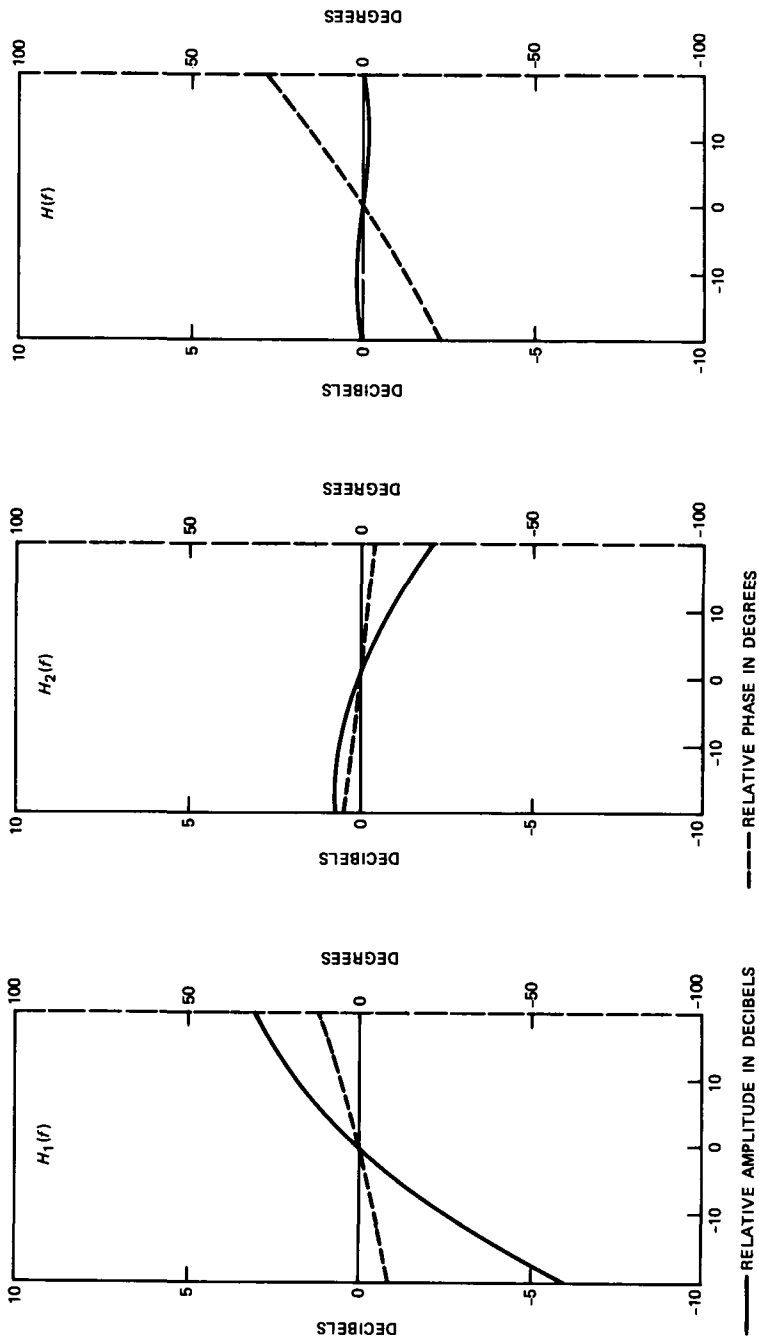

Fig. 2—Relative amplitude and phase plots for $H_1(f)$ and $H_2(f)$, corresponding to Case 1 in Table I, and the resulting combiner output response, $H(f)$, when β_1 and β_2 are derived using the control scheme in Fig. 1; no noise present. The plots cover a 40-MHz bandwidth and, for convenience, all magnitudes and phases are shifted so as to be zero at band center.

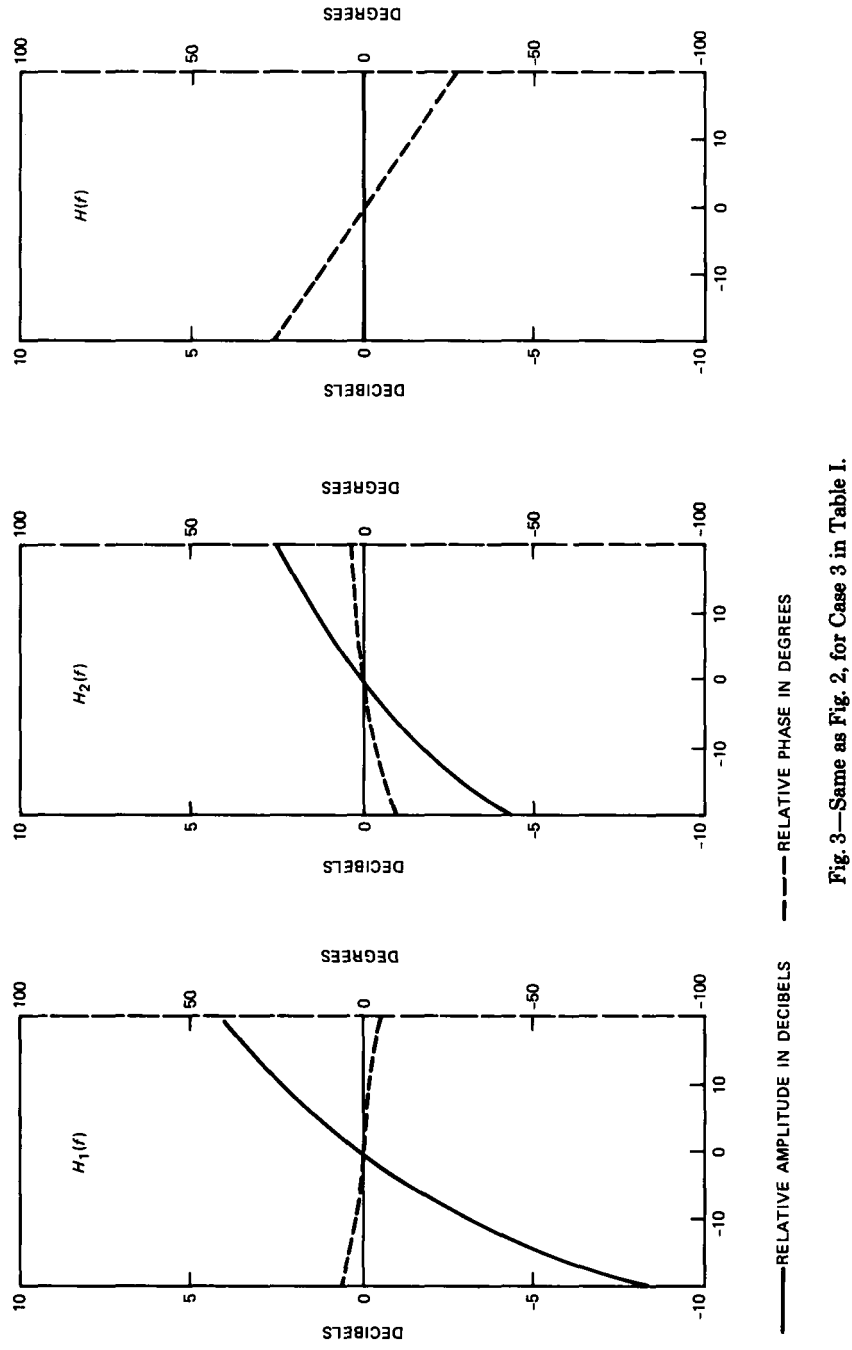

Fig. 3—Same as Fig. 2, for Case 3 in Table I.

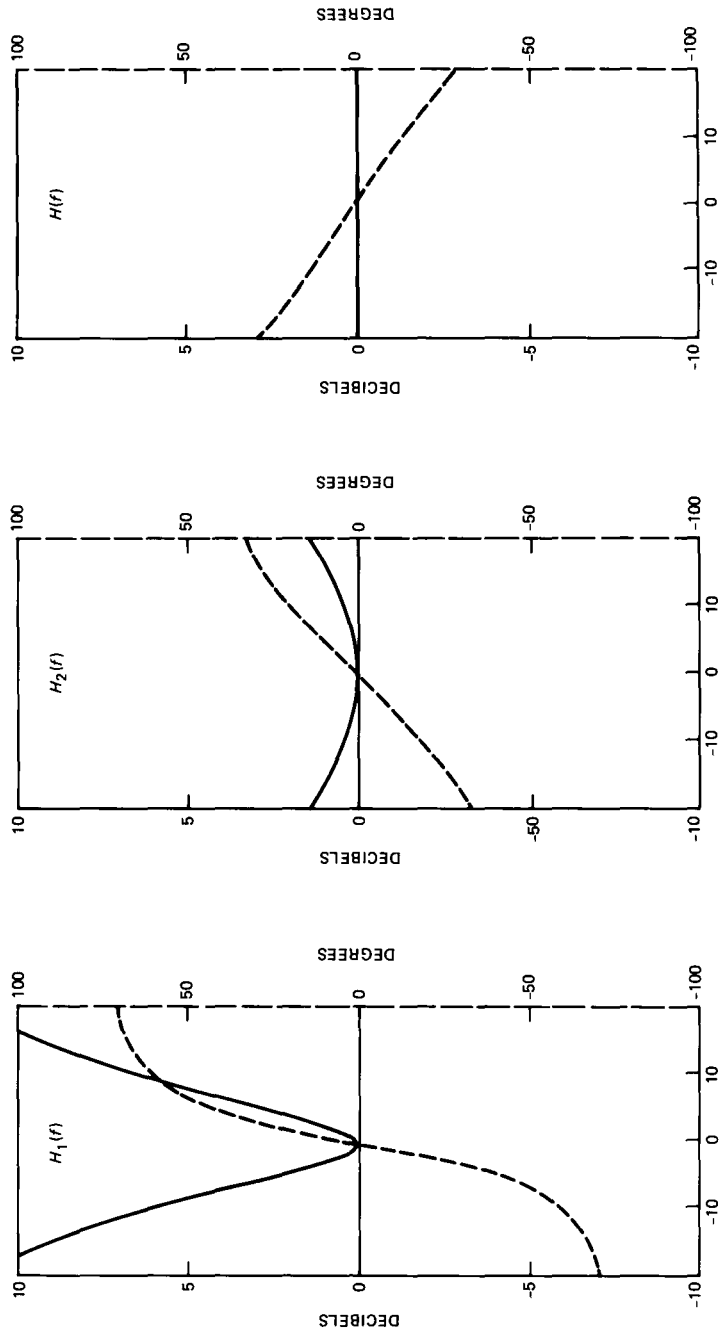

Fig. 4—Same as Fig. 2, for Case 4 in Table I.

Table II—Combiner performance results for CNR = 60 dB

	Detection Measure (in dB)				Decibel Range of $\|H(f)\|$			
Case	Γ_1	Γ_2	Γ_3	Γ_4	R_1	R_2	R_3	R_4
1	43.80	42.67	11.12	20.88	0.11	0.062	9.34	2.77
2	46.99	46.99	46.99	11.15	0.006	0.0	0.0	9.79
3	36.06	35.62	9.17	13.39	0.21	0.14	12.25	6.82
4	53.13	53.12	6.82	25.91	0.002	0.001	11.35	1.39
5	29.23	27.60	2.80	3.02	0.37	0.27	16.96	16.49
6	35.32	34.99	18.21	5.38	0.26	0.21	3.19	19.09
7	42.28	40.72	18.31	17.80	0.11	0.13	3.76	3.08
8	63.84	59.24	10.70	29.02	0.006	0.022	7.38	1.06

Table III—Combiner performance results for CNR = 40 dB

	Detection Measure (in dB)				Decibel Range of $\|H(f)\|$			
Case	Γ_1	Γ_2	Γ_3	Γ_4	R_1	R_2	R_3	R_4
1	41.01	40.43	11.12	20.86	0.11	0.06	9.34	2.77
2	27.46	26.99	26.99	11.15	0.44	0.0	0.0	9.79
3	29.91	29.60	9.16	13.39	0.41	0.18	12.25	6.82
4	33.38	33.33	6.77	25.51	0.11	0.05	11.35	1.39
5	27.11	25.70	2.79	3.00	0.40	0.27	16.96	16.49
6	31.29	30.97	18.13	5.37	0.36	0.21	3.19	19.09
7	38.08	37.72	18.30	17.71	0.17	0.13	3.76	3.08
8	46.23	46.00	10.68	28.96	0.022	0.014	7.38	1.06

Table IV—Combiner performance results for CNR = 20 dB

	Detection Measure (in dB)				Decibel Range of $\|H(f)\|$			
Case	Γ_1	Γ_2	Γ_3	Γ_4	R_1	R_2	R_3	R_4
1	25.98	25.76	10.68	19.67	0.58	0.43	9.34	2.77
2	12.91	12.54	6.99	10.96	5.72	4.31	0.0	9.79
3	14.68	14.35	8.29	12.93	3.96	2.85	12.25	6.82
4	15.67	15.63	3.58	15.64	1.54	1.37	11.35	1.39
5	11.72	11.68	1.97	2.19	2.16	1.83	16.96	16.49
6	15.21	15.14	13.49	4.76	1.99	1.62	3.19	19.09
7	23.80	23.74	17.69	12.75	0.75	0.63	3.76	3.08
8	27.63	27.63	9.09	25.41	0.22	0.20	7.38	1.06

with "suboptimal" space diversity combining would generally perform much better than one using no diversity (Γ_3 or Γ_4) or selection diversity (the larger of Γ_3 and Γ_4).

2. Comparing Γ_2 with Γ_1 reveals that the "suboptimal" combiner would perform nearly as well as the "optimal" one, at least for the response pairs considered here.

3. For the "suboptimal" combiner, the range (R_2) of the post-

combiner frequency response is generally much smaller than that for either branch alone (R_3 and R_4). It is also comparable to that for "optimal" combining (R_1), often being even smaller.

4. Comparing Tables II, III, and IV reveals the trends of combiner performance as CNR decreases from high values (≥40 dB) to low ones (20 dB). At high values, the combiner emphasizes minimum dispersion, as reflected in the data for R; at low values, combiner action aims more at minimizing noise and so dispersion reduction is limited.

It thus appears that the noncoherent measurement/control scheme described here would be effective in *any* receiver situation. This includes receivers *without* post-combiner equalization, wherein Γ should be maximal to optimize detection; and receivers *with* equalization, wherein R should be minimal to facilitate equalizer convergence. It is clear that both aims are served by the same algorithm. Moreover, the scheme is simple, fast-acting, and operates in proximity to the combining circuitry.

Some issues remain to be settled. One is whether the search algorithm will always converge to either the near-optimal solution or to one that, in any case, yields very good performance. The results obtained for our limited sampling of response pairs offer encouragement on this score. Another issue concerns the effectiveness of diversity combining over a statistical *ensemble* of fading conditions, that is, we have obtained results here for just eight selected response pairs. In a separate study, however, we invoked a recently developed statistical model for dual-diversity channels[20,21] to simulate a large population (ensemble) of response pairs ($H_1(f)$, $H_2(f)$), and we obtained probability distributions for Γ and R over that population. The results are reported in a companion paper.[22]

REFERENCES

1. C. W. Anderson, S. G. Barber, and R. N. Patel, "The Effect of Selective Fading on Digital Radio," IEEE Trans. Commun., *COM-27*, No. 12 (December 1979), pp. 1870–75.
2. S. Komaki et al., "Characteristics of a High Capacity 16 QAM Digital Radio System in Multipath Fading," IEEE Trans. Commun., *COM-27*, No. 12 (December 1979), pp. 1854–61.
3. Y. Y. Wang, "Simulation and Measured Performance of a Space Diversity Combiner for 6 GHz Digital Radio," IEEE Trans. Commun., *COM-27*, No. 12 (December 1979), pp. 1896–907.
4. S. Komaki, Y. Okamoto, and K. Tajima, "Performance of 16-QAM Digital Radio System Using New Space Diversity," Paper 52.2, Int. Conf. Commun., June 8–12, 1980, Seattle, Washington.
5. T. Murase, K. Morita, and S. Komaki, "200 Mb/s 16-QAM Digital Radio System with New Countermeasure Techniques for Multipath Fading," Paper 46.1, Int. Conf. Commun., June 14–18, 1981, Denver, Colorado.
6. P. Hartmann and B. Bynum, "Design Consideration for an Extended Range Adaptive Equalizer," Paper 46.5, Int. Conf. Commun., June 14–18, 1981, Denver, Colorado.
7. A. J. Giger and W. T. Barnett, "Effects of Multipath Propagation on Digital Radio," IEEE Trans. Commun., *COM-29*, No. 9 (September 1981), pp. 1345–52.

8. P. D. Karabinis, "Maximum-Power and Amplitude-Equalizing Algorithms for Phase Control in Space Diversity Combining," B.S.T.J., *62*, No. 1, Part 1 (January 1983), pp. 63–90.
9. R. Iyer et al., "Effects of Space Diversity Reception on Multipath Induced Distortions in Terrestrial Microwave Channels," Paper 3.B.5, Int. Conf. Commun., June 13–17, 1982, Philadelphia, PA.
10. A. Ricagni and T. Testi, "IF Combining Techniques for Space Diversity in Analog and Digital Radio Systems," Paper 4.B.6, Int. Conf. Commun., June 13–17, 1982, Philadelphia, PA.
11. R. A. Nichols, "An IF Combiner for Digital and Analog Radio Systems," Paper 4.B.7, Int. Conf. Commun., June 13–17, 1982, Philadelphia, PA.
12. L. J. Greenstein and B. A. Czekaj, "A Polynomial Model for Multipath Fading Channel Responses," B.S.T.J., *59*, No. 7 (September 1980), pp. 1197–225.
13. L. J. Greenstein and B. A. Czekaj, "Modeling Multipath Fading Responses Using Multitone Probing Signals and Polynomial Approximation," B.S.T.J., *60*, No. 2 (February 1981), pp. 193–214.
14. W. C. Wong and L. J. Greenstein, unpublished work.
15. R. W. Lucky, J. Salz, and E. J. Weldon, Jr., *Principles of Data Communication*, New York, NY: McGraw-Hill, 1968, Chapter 6.
16. B. Widrow, "A Comparison of Adaptive Algorithms Based on the Methods of Steepest Descent and Random Search," IEEE Trans. Ant. and Prop., *AP-24*, No. 5 (September 1976), pp. 615–37.
17. W. C. Wong and L. J. Greenstein, "Multipath Fading Models and Adaptive Equalizers in Microwave Digital Radio," IEEE Trans. Commun., *COM-32*, No. 8 (August 1984), pp. 928–34.
18. G. J. Foschini and J. Salz, "Digital Communications Over Fading Radio Channels," B.S.T.J., *62*, No. 2, Part 1 (February 1983), pp. 429–56.
19. A. Gersho, "Adaptive Equalization of Highly Dispersive Channels for Data Transmission," B.S.T.J., *48*, No. 1 (January 1969), pp. 55–70.
20. W. D. Rummler, "A Statistical Model of Multipath Fading on a Space Diversity Radio Channel," B.S.T.J., *61*, No. 9, Part 1 (November 1982), pp. 2185–219.
21. W. D. Rummler, "A Rationalized Model for Space and Frequency Diversity Line-of-Sight Radio Channels," Paper E2.7, Int. Conf. Commun., June 19–22, 1983, Boston, MA.
22. L. J. Greenstein and Y. S. Yeh, "A Simulation Study of Space Diversity and Adaptive Equalization in Microwave Digital Radio," AT&T Tech. J., this issue.

AUTHORS

Larry J. Greenstein, B.S.E.E., 1958, M.S.E.E., 1961, and Ph.D. (Electrical Engineering), 1967, Illinois Institute of Technology; AT&T Bell Laboratories, 1970—. Mr. Greenstein currently heads the Radio Systems Research Department at Crawford Hill in Holmdel, NJ. His most recent work has dealt with communications satellites, mobile telephony, and microwave digital radio. His previous work was on digital encoding, digital filtering, and, at IIT Research Institute before 1970, airborne radar. Member, Eta Kappa Nu, Tau Beta Pi, and Sigma Xi; Senior Member, IEEE; Senior Technical Editor, IEEE Communications Magazine; co-recipient, IEEE Communications Society's 1984 Prize Paper Award in Communications Systems.

Yu-Shuan Yeh, B.S.E.E., 1961, National Taiwan University; M.S.E.E., 1964, Ph.D., 1966, University of California, Berkeley, CA; Harvard University, 1966–67; AT&T Bell Laboratories, 1967—. From 1961 to 1962, Mr. Yeh was an electronics officer in the Chinese Navy. He was a Research Fellow at Harvard University from 1966 to 1967 doing antenna research. In 1967 he joined AT&T Bell Laboratories and is currently a Supervisor in the Network Systems Research Department. His research interests include satellite communications, mobile radio, microwave digital radio, and data networks. Mr. Yeh holds over a dozen patents and is the recipient of two best paper awards from IEEE Transactions. Fellow, IEEE.